Journal of *Marine Science and Engineering*

MDPI

Article

ShipNetSim: An Open-Source Simulator for Real-Time Energy Consumption and Emission Analysis in Large-Scale Maritime Networks

Ahmed Aredah and Hesham A. Rakha *

Center for Sustainable Mobility, Virginia Tech, Blacksburg, VA 24061, USA; ahmedaredah@vt.edu
* Correspondence: hrakha@vt.edu

Abstract: The imperative of decarbonization in maritime shipping is underscored by the sector's sizeable contribution to worldwide greenhouse gas emissions. ShipNetSim, an open-source multi-ship simulator created in this study, combines state-of-the-art hydrodynamic modeling, dynamic ship-following techniques, real-time environmental data, and cybersecurity threat simulation to quantify and evaluate marine fuel consumption and CO_2 emissions. ShipNetSim uses well-validated approaches, such as the Holtrop resistance and B-Series propeller analysis with a ship-following model inspired by traffic flow theory, augmented with a novel module simulating cyber threats (e.g., GPS spoofing) to evaluate operational efficiency and resilience. In a case study simulation of the journey of an S175 container vessel from Savannah to Algeciras, the simulator estimated the total fuel consumption to be 478 tons of heavy fuel oil and approximately 1495 tons of CO_2 emissions for a trip of 7 days and 15 h within 13.1% of reported operational estimates. A twelve-month sensitivity analysis revealed a marginal 1.5% range of fuel consumption variation, demonstrating limiting variability for different environmental conditions. ShipNetSim not only yields realistic predictions of energy consumption and emissions but is also demonstrated to be a credible framework for the evaluation of operational scenarios—including speed adjustment, optimized routing, and alternative fuel strategies—that directly contribute to reducing the marine carbon footprint. This capability supports industry stakeholders and policymakers in achieving compliance with global decarbonization targets, such as those established by the International Maritime Organization (IMO).

Keywords: ShipNetSim; ship large-scale simulation; ship longitudinal motion; ship energy consumption; ship environmental footprint

Received: 7 February 2025
Revised: 21 February 2025
Accepted: 6 March 2025
Published: 8 March 2025

Citation: Aredah, A.; Rakha, H.A. ShipNetSim: An Open-Source Simulator for Real-Time Energy Consumption and Emission Analysis in Large-Scale Maritime Networks. *J. Mar. Sci. Eng.* **2025**, *13*, 518. https://doi.org/10.3390/jmse13030518

1. Introduction

This paper introduces an open-source simulator tailored for modeling long-voyage cargo ships navigating large-scale maps. The simulator, named ShipNetSim (Ship Network Simulator), enables interactions between ships while providing real-time energy consumption data, facilitating the estimation of their carbon footprint. ShipNetSim is specifically designed to predict energy consumption and greenhouse gas (GHG) emissions for ships. The simulator operates with a single degree of freedom in its ship modeling, a limitation intentionally chosen to achieve a significant reduction in computational simulation time while maintaining accurate energy consumption estimates.

In addition to providing a comprehensive energy consumption analysis, ShipNetSim serves as a tool for informing policymaking in maritime operations. The simulator's ability to model different operational scenarios—such as optimized routing and speed

adjustments—allows shipping companies and regulatory bodies to assess compliance with international carbon-reduction targets set by organizations like the International Maritime Organization (IMO). By giving insight into strategies for reducing emissions, ShipNetSim can support stakeholders in adapting to changing environmental regulations and perhaps creating these regulations.

In addition to emissions concerns, the increasing digitization of the maritime industry necessitates special attention to cyber threats, particularly for systems relying on real-time data and automation. As modern vessels incorporate advanced technology for navigation, propulsion, and communication, they become susceptible to a range of cyberattacks, such as GPS spoofing. ShipNetSim has functionalities of modeling possible cyberattacks. Such scenarios serve to evaluate the impacts of both cybersecurity threats on ship navigation, energy efficiency, and operational safety, and as such, it has provided a good basis for testing the operating and security vulnerabilities of modern maritime systems.

The critical need for decarbonization in shipping is highlighted by the significant levels of greenhouse gas emissions caused by this industry. Accordingly, the development of new simulation tools is essential to investigate methods of lowering both fuel consumption and CO_2 emissions. ShipNetSim meets this requirement by facilitating the assessment of various operational measures—such as the utilization of alternative fuels, hybrid propulsion systems, and route optimization—aimed at reducing the overall carbon footprint of shipping operations. By providing quantitative estimates of emission savings, ShipNetSim is a vital tool for informing both operational optimization and policy-making to decarbonize shipping.

Following the Introduction, Section 2 presents the Literature Review. In Section 3, we outline the novelty and contributions of ShipNetSim. Section 4 details the simulation model, including the mathematical formulations for ship dynamics and resistance calculations. Section 5 describes the simulator's architecture and operational workflow. In Section 6, we present case studies that validate the simulator's performance, and finally, Section 7 concludes the paper and outlines future research directions.

2. Literature Review

The maritime sector is facing an unprecedented transformation motivated by the necessity to save energy and lower carbon emissions. This has led to the evolution of ship simulators for energy consumption analysis. This literature review consolidates existing research in this field, focusing on conceptualizing the ShipNetSim simulator, a new simulator for simulating large cargo vessels with particular consideration of energy consumption prediction and carbon footprint.

Ship simulators have evolved from simple movement prediction tools to more capable systems for simulating serveral aspects of maritime operations. For instance, a computational fluid dynamics (CFD) based simulation model was conducted by [1] on unsteady motion of ships in waves, focusing on the added resistance and performance in wave conditions. Ref. [2] developed a low-complexity ship-movement simulator offering a system that adapts to different ship shapes and engines in different sea conditions. Authors in [3] developed a simulator to predict ship maneuvering behavior under normal wave conditions. They used a two-time scale model in their study to separate the effects of maneuvering motions and those resulting from wave action. The simulators were originally concerned only with ship navigation, excluding energy consumption or carbon emission analysis. But with increased focus on environmental regulations and sustainable issues, simulator application has been further developed. This change demonstrates an increasing demand for tools that not only forecast ship navigation but also take into account energy efficiency and emissions.

Building on these early movement-focused efforts, modern simulators have expanded to address not only navigation but also energy and emissions modeling. For instance, the IMO's carbon-reduction targets have prompted the development of simulators to support policy-makers in designing efficient maritime regulations. Simulators such as ShipNetSim support international compliance with environmental regulations by simulating energy-efficient operating scenarios, thus helping attain sustainability in the maritime industry. These simulations respond to policy initiatives such as the IMO's Greenhouse Gas Strategy setting, clear goals for a reduction in CO_2 emissions by 2050. Recent advancements in simulation frameworks have further enhanced the ability to optimize ship energy systems. The Design Lab framework, introduced by Yum et al. (2024), provides a simulation-based approach that integrates operational profiles, vessel performance metrics, and system evaluations to improve energy efficiency and sustainability in maritime transport [4].

As the digital transformation of maritime operations grows, so too does the need for simulators that integrate both cybersecurity and operational efficiency. Addressing these challenges, recent studies similar to [5] have focused on the growing importance of cybersecurity and cyber threats to ship systems and proposed a multi-purpose cyber-environment simulator for testing system vulnerabilities in real time. Meanwhile, Ref. [6] developed the Cyber-SHIP Lab, which develops research capabilities in maritime cyber threats by providing the tools to counter threats, such as those from GPS spoofing or system breaching. Addressing the needs for both cybersecurity and policy-making, Ref. [7] presented a decision support system, which merged cyber risk and econometric models to train port stakeholders efficiently in responding against cyber threats. Their system focused on the interaction between security and efficiency within the maritime domain. Moreover, Ref. [8] demonstrated holistic cyber defense approaches for maritime logistics and further underlined the need for the integration of cyber resilience within maritime simulators.

Advancements in route planning and its optimization have also shaped the evolution of such simulators, as efficient navigation is critical for reducing fuel consumption and minimizing environmental impact. These methods also complement energy and emission predictions by improving overall ship efficiency. The research done by [9] performed an optimal ship routing simulation for a bulk carrier. Their research evaluated the impact of rough sea voyages and speed loss analysis, incorporating environmental factors such as wind conditions in simulating realistic ship movements. Ref. [10] proposed a path planning approach for autonomous navigation. Their research employed Q-learning to optimize ship movements without any human input. Ref. [11] introduced a method for automated ship navigation, highlighting the capabilities of autonomous route optimization and collision avoidance in challenging navigation environments. Despite these studies focusing on navigation and routing, ship characteristics involvement was very limited in their optimization.

Recent simulators and models have specifically targeted energy consumption predictions, which are critical for reducing operational costs and aligning with environmental policies. For example, the authors in [12] developed the ship impact model (SIM) for assessing carbon dioxide reduction technology at an early design stage. This model demonstrates the potential for significant fuel consumption and carbon emissions reduction. Their research does not address operational aspects such as route optimization and real-time energy management. Ref. [13] estimated maritime transport fuel consumption using the Response Surface Methodology. Their study offered a statistical approach to model fuel consumption. However, this method does not incorporate real-time data or dynamic environmental conditions. Ref. [14] highlighted the significance of incorporating energy-efficient operational training into ship simulators, demonstrating the potential for achieving up to a 10% reduction in fuel consumption. Ref. [15] investigated carbon emissions for cargo ships

through process simulations, highlighting the techno-economic challenges and potential for CO_2 reduction. Ref. [16] carried out simulations to explore strategies for mitigating carbon emissions at container terminals. Their research emphasized the importance of speed reduction and alternative fuels in reducing carbon emissions. Ref. [17] develops a model to simulate the marine diesel engines with an emphasis on emission predictions. The model was calibrated against experimental data. However, they did not integrate it with a complete ship simulator. Furthermore, waste heat recovery has gained traction as a viable method for improving ship energy efficiency. Lebedevas and Čepaitis (2024) demonstrated that by integrating Organic Rankine Cycle (ORC) technology with marine diesel engines, ship efficiency could be increased by up to 21%, significantly reducing fuel consumption and emissions [18].

More integrated simulators have addressed some of the gaps in previous simulators. For example, Ref. [19] proposed a Bayesian forecasting method to extrapolate ship movements and emissions. The study lacks real-time adjustments by changing environmental conditions. Ref. [20] reviews the engine control strategies in waves towards greenhouse gas emissions. The paper still misses a comprehensive approach taking all elements of the ship dynamics. These studies mark a significant step towards bridging the gap of integrating energy and emission considerations within ship simulations. Recent advancements have also explored integrating carbon capture technologies within ship simulation frameworks. Hai et al. (2024) proposed an innovative system combining natural gas engines with carbon capture storage (CCS) to enhance energy efficiency while reducing emissions. Their study emphasized how exhaust heat recovery strategies can optimize ship energy use while maintaining compliance with stringent IMO decarbonization targets [21]. Further innovations in maritime propulsion have demonstrated the effectiveness of integrating renewable energy technologies into LNG carriers. Ammar and Seddiek (2025) explored the use of Flettner rotor-assisted propulsion for LNG vessels, showing that by utilizing six rotors, fuel savings of 3.49% to 4.49% could be achieved, while overall energy efficiency improved by 4.68%. These results highlight how hybrid propulsion methods can significantly contribute to decarbonization goals [22]. However, there remains a gap in integrating such methodological analysis in ship simulators, especially large cargo ship simulators, with a comprehensive focus on both energy consumption and carbon emissions, which ShipNetSim aims to address.

3. Novelty and Contributions

ShipNetSim distinguishes itself from existing maritime simulation tools through a set of innovative features and integrative methodologies. Its novelty and contributions can be summarized as follows:

3.1. Comprehensive Multi-Domain Simulation

ShipNetSim is the very first open-source simulator that takes into account real-time energy consumption, greenhouse gas emissions, and cybersecurity implications simultaneously over large maritime networks. In contrast to conventional simulators that address either ship movement or energy efficiency separately, ShipNetSim encompasses:

- Propulsion and Resistance Modeling: ShipNetSim utilizes advanced hydrodynamic models such as Holtrop method and B-Series thrust and torque coefficients to model the resistance forces on a ship with high accuracy under different environmental conditions.
- Dynamic Ship-Following Models: The simulator, incorporating principles of traffic flow theory, possesses an advanced ship-following model that takes into consideration vessel spacing, operators' response delays, and braking dynamics, thus simulating longitudinal behavior realistically.

- Path Finding and Interaction with the Environment: Supported by a visibility graph data structure combined with QuadTree indexing, ShipNetSim simulates path planning through complicated maritime environments effectively, with the incorporation of variable environment parameters (such as wave properties and wind resistance).
- Cybersecurity Simulation: A new module simulates cyber threats like GPS spoofing, network attacks, and signal jamming to challenge the resilience of maritime operations to cyber disruptions.

3.2. Real-Time, Data-Driven Analysis

ShipNetSim is the only one to use real-world environmental data (e.g., geospatial TIFF files) to inform its calculations of resistance and energy consumption. This dynamic methodology enables the simulator to:

- Provide real-time measurement of energy use and emissions.
- Enable sensitivity analyses through examination of how monthly environmental changes contribute to operational effectiveness.
- Offer actionable suggestions for optimizing ship performance in different operating conditions.

3.3. Relevance to Decarbonisation and Policy Adherence

With increasing regulatory and societal pressure for decarbonization of maritime transport, ShipNetSim becomes a critical decision-supporting tool, in terms of:

- Quantification of different operational measures impacts, such as speed adjustments, optimized routing, or alternative fuel utilization, on fuel consumption and CO_2 emissions.
- Scenario analysis that enables companies to adhere to global decarbonization targets (such as those established by the IMO) by examining emission reduction strategies and their effectiveness.
- An experimental platform for innovative decarbonization measurements, for example, introducing renewable energy sources or hybrid propulsion systems. This thus supports operational improvements and policy formulation.

3.4. Modularity, Extensibility, and Future Communication Capabilities

With its modular architecture, ShipNetSim is not only extremely robust in its present capabilities but also extremely extensible. Future directions for research include:

- Lateral Dynamics Integration: An extension of the simulation framework to model lateral movements of ships and more intricate maneuvering patterns.
- Advanced Cyber Threat Frameworks: Incorporating machine learning algorithms for predictive analytics to enable cybersecurity evaluations to be more impactful.
- Better Energy Modeling: Incorporating auxiliary systems, additional fuel types, and more extensive engine performance readings.
- Communication Between Vessels and Shore Facilities: There is a need to develop modules that enable real-time interactions between maritime vessels and also between vessels and shore facilities. These capabilities would enable synchronized navigation, adaptive decision-making processes, and timely emergency responses, thus enhancing the operational realism and feasibility of the simulator.

3.5. Validation and Practical Impact

ShipNetSim was validated through an extensive case study of S175 container ship trade between Savannah and Algeciras. The simulator was found to have a satisfactory correlation with fuel consumption and emission estimates reported (within 13.1% error), demonstrating its real-life feasibility for:

- Operational optimization and route planning.
- Environmental impact assessments.
- Strategic planning for decarbonization in maritime transport.

4. Simulation Model

The simulator has three main components; propulsion-resistance models, ship co-existence model, and path finding. The following sections will explore each one separately. The Abbreviation lists all the variables used in the model. The dynamics model is further explained in [23–25].

4.1. Propulsion-Resistance Models

This section is based mainly on the work done by [26] where the calm-water ship resistances are calculated using the Holtrop method and the performance of the propeller is modelled using the B-Series thrust and torque coefficients (the user has the flexibility to use custom coefficients). In addition to the calm water resistance, the wave and wind resistances are estimated using the models proposed by [27,28].

The total resistance $R_t(t)$ on the ship at time t is divided into the calm-water resistance $R_{CALM}(t)$, added resistance due to wave $R_{AW}(\omega(t)|u(t), \beta(t))$ and wind $R_{AA}(t)$:

$$R_{t|n}(t) = R_{CALM}(t) + R_{AW}(\omega(t)|u(t), \beta(t)) + R_{AA}(t) \tag{1}$$

where $\omega(t)$, $u(t)$, and $\beta(t)$ are the wave frequency in hz, vessel speed in m/s, and the wave relative heading angle, respectively.

$$R_{CALM}(t) = R_F(t) \cdot (1 + k_1) + R_W(t) + R_B(t) + R_{TR}(t) + R_A(t) \tag{2}$$

where $R_F(t), R_W(t), R_B(t), R_{TR}(t),$ and $R_A(t)$ are the frictional, wave-making, bulbus bow, the transom, and the model correction resistances, respectively, at time t. k_1 is the form factor of the ship.

The added resistance due to wind $R_{AA}(t)$ is dependent on the area of structure above the waterline as well as the relative wind speed [29]. The R_{AA} is estimated using Equation (3) provided by [30].

$$R_{AA} = \frac{1}{2}\rho_A C_{AA}(\psi(t)) A_{XV} V_{WR}^2 \tag{3}$$

where ρ_A is the air density in kg/m^3, A_{XV} is the transverse projected area above waterline including superstructures in m^2, V_{WR} is the relative wind speed in m/s, ψ is the relative wind direction, C_{AA} are the wind resistance coefficients for various heading angles. The C_{AA} is estimated using Equation (4) provided by [28]:

$$\begin{aligned} C_{AA|X} &= X_0 + X_1 \cos\psi(t) + X_3 \cos 3\psi(t) + X_5 \cos 5\psi(t) \\ C_{AA|Y} &= Y_1 \sin\psi(t) + Y_3 \sin 3\psi(t) + Y_5 \sin 5\psi(t) \end{aligned} \tag{4}$$

where $C_{AA|X}$ and $C_{AA|Y}$ are the wind resistance coefficients in the longitudinal and lateral directions.

For the wave resistance prediction, in this research, we use the the model proposed by [27,30]. However, since the ShipNetSim is adopting a modular structure framework, using any other prediction model is also allowed. The total added wave resistance is a sum of two components, added resistance due to wave reflection $R_{awr}(\omega(t)|u(t), \beta(t))$, and due to ship motions $R_{awm}(\omega(t)|u(t), \beta(t))$ [31] and can be expressed as follows:

$$R_{AW}(t) = R_{awr}(\omega(t)|u(t),\beta(t)) + R_{awm}(\omega(t)|u(t),\beta(t)) \tag{5}$$

The wave reflection component is calculated as:

$$R_{awr}(\omega(t)|u(t),\beta(t)) = R_{awr}(\omega(t)|u(t),0)\cdot Fr(t)^{X}\cos\beta(t),$$
$$\text{where } X = \begin{cases} (\lfloor z(t)\cos\beta(t)\rfloor - \lceil\cos\beta(t)\rceil)Fr(t), & \text{for } 0 \le \beta(t) \le \frac{\pi}{2} \\ -1.5(\lfloor\cos\beta(t)\rfloor + \lceil\cos\beta(t)\rceil)Fr(t), & \text{for } \frac{\pi}{2} < \beta(t) \le \pi \end{cases} \tag{6}$$

and the added resistance component due to ship motions is calculated as:

$$\begin{aligned} R_{awm}(\omega(t)\mid u(t),\beta(t)) = {} & R_{awm}(\omega(t)\mid u(t),0)\cdot e^{-\left(\frac{\beta(t)}{\pi}\right)^{4\sqrt{Fr}}} \\ & + \rho_w g\zeta_a(t)^2 B^2/L_{pp}\left[\frac{\lambda(t)}{B}\cdot\max(\cos\beta(t),0.45)\right]^{-6Fr}\sin\beta \end{aligned} \tag{7}$$

On the other hand, thrust force and torque generated by the propeller, rotating with a speed of n, are required to be determined in order to solve equations of motion in surge direction. B-series is assumed to calculate the thrust and torque coefficients. The thrust coefficient is calculated as:

$$K_T = \frac{T_p}{\rho_w n^2 D^4} \tag{8}$$

The Torque coefficient is defined as:

$$K_Q = \frac{Q_p}{\rho_w n^2 D^5} \tag{9}$$

where D is the propeller diameter (m), ρ_W is the water density (kg/m^3), n is the rotational speed of the propeller (rad/s). The efficiency of the propeller is calculated by:

$$\eta = \frac{K_t}{K_Q}\frac{J}{2\pi} \tag{10}$$

The ship's propulsion force is determined using Equation (11). This model accounts for both the fundamental propulsion forces and the maximum force the system can sustain. Additionally, the throttle function is discretized following the previously outlined methodology.

$$F_t(t) = \sum_l \left(\frac{1000\eta_n\lambda(t)P_l^{\max}}{u(t)}\right) \tag{11}$$

where $P_l^{\max}$ is the current engine's max power. This power is initially set to the Specified Maximum Continuous Rating ($SMCR$) point, which lies within the region defined by lines L1-L2-L3-L4 on the engine layout curve (see Figure 1). This $SMCR$ point is calculated based on the maximum design speed of the ship and its associated resistance forces as defined by the below equation:

$$SMCR_{power} = PD_{power} \times \frac{\frac{100+SM}{100}}{\frac{100-EM}{100}} \tag{12}$$

$$SMCR_{speed} = PD_{speed} \times \left(\frac{SMCR_{power}}{PD_{power}}\right)^{1/3} \times \left(1 - \frac{LRM}{100}\right) \tag{13}$$

where SM, EM, and LRM are the sea margin, engine margin, light running margin, respectively. The typical values are 15%, 10%, and 6%, though these parameters can be

customized by the user. The value of $P_l^{\max}$ is calculated by finding the equilibrium point between the engine and the propeller power curves (estimated by Equations (8)–(10)). The engine power curve can be estimated by the power-performance function below [32]:

$$P(RPM) = 0.87\frac{P_M}{RPM_M} \cdot RPM + 1.13\frac{P_M}{RPM_M^2} \cdot RPM - 1.0\frac{P_M}{RPM_M^3} \cdot RPM \tag{14}$$

where P_M and RPM_M are the maximum power and speed of the engine which corresponds to SMCR and $P(RPM)$ is the power at the given RPM.

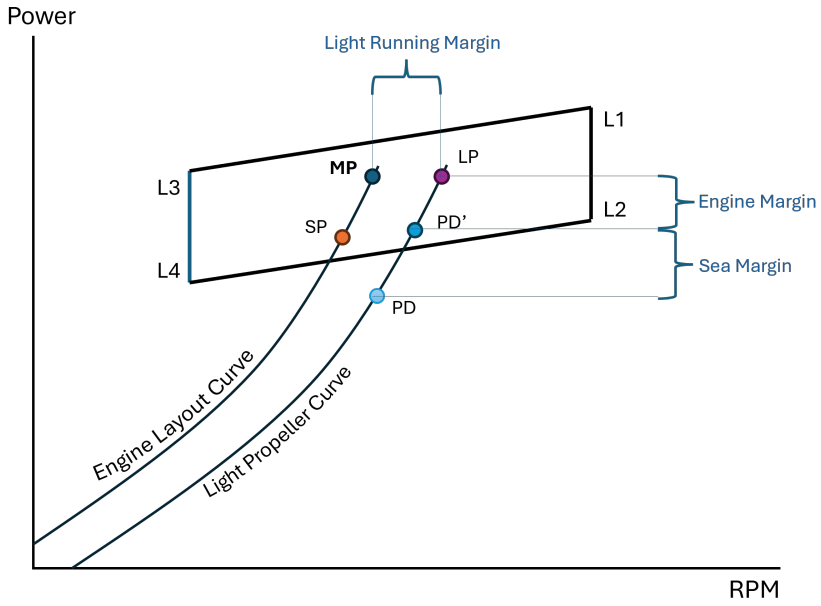

Figure 1. Engine layout curve.

In addition, the ship may operate at the corner points of the engine safe zone. In such case, the default is the economic power point of the engine which corresponds to power point L2 in the engine layout curve. If the speed is reduced by 20% of the max speed due to increased resistance, the engine transitions to higher power points (L3 or L1) sequentially. Additionally, λ is the thrust level that moves the engine power along its power curve and is calculated by:

$$\lambda_n(t) = \begin{cases} \dfrac{\frac{u_n(t)}{u_d(t)}}{t_1 + \frac{t_2}{1-\frac{u_n(t)}{u_d(t)}} + t_3\frac{u_n(t)}{u_d(t)}}, & 0 \leqslant u_n(t) \leqslant u_m(t) \\ \max\left(\dfrac{\frac{u_n(t)}{u_d(t)}}{t_1 + \frac{t_2}{1-\frac{u_n(t)}{u_d(t)}} + t_3\frac{u_n(t)}{u_d(t)}}, \lambda^*\right), & u_m(t) \leqslant u_n(t) \leqslant u_d(t) \end{cases} \tag{15}$$

The variables t_1, t_2, and t_3 are calibration coefficients initially introduced in [33] and later refined in [34]. These parameters are derived based on the observation that only about 60% of a vehicle's motor capacity is typically utilized, rather than its full power. However, this assumption does not hold for ships, as the model incorporates dynamic P_l^{max} to account for full power usage. Consequently, these coefficients are recalibrated to represent the complete utilization of ship power, with the recommended values being 0.001, 0.050, and 0.030, respectively.

This is further enhanced by ShipNetSim's thrust allocation strategy, designed to optimize fuel consumption by dynamically adjusting throttle settings based on the equilibrium between engine power and propeller RPM (as described earlier). The simulation calculates

the optimal throttle level by finding the equilibrium point where the engine's power output matches the propeller's resistance, ensuring efficient energy use. This equilibrium is achieved by considering both the engine's performance curve and the propeller's thrust and torque coefficients, calculated using the B-Series method. At each time step, ShipNet-Sim adjusts the throttle to maintain this balance, taking into account the current operating conditions such as ship speed, environmental resistance (waves, wind), and the desired route. The simulator can also respond to external factors, such as increased resistance due to rough seas, by increasing the throttle to maintain speed or reducing it to save fuel when lower speeds are acceptable. These adjustments help optimize fuel consumption and reduce emissions, especially when operating in conditions where the engine is running at less than full capacity. This real-time adjustment ensures that the engine operates within its most fuel-efficient range, contributing to lower overall energy consumption and a more environmentally friendly voyage.

4.2. Ship Motion and Coexisting Models

This section presents a proposed model for ship-following dynamics incorporating external forces such as resistance and propulsion forces. Additionally, the model integrates the operator's reaction delay and the inherent time lag in the activation of the ship's stopping mechanism. This formulation generates a time-dependent profile of the ship's acceleration as a function of the spacing between vessels and the relative velocities of the leading and following ships at discrete time steps.

The model calculates the maximum acceleration $a_n^{max}(t)$ of a ship by considering the difference between propulsion $F_n(t)$ and resistance forces $R_n(t)$ relative to its total mass m_n (as shown in Equation (16)). The ship's total mass includes the vessel's lightweight, cargo weight, and surge-added mass. According to [35], the surge-added mass can be determined using Equation (17), where ∇ represents the ship's displacement volume, and K_1, the added mass coefficient, is derived from Equation (18). The coefficient K_1 depends on α_0, which is calculated using Equation (19). The eccentricity, e, needed for this calculation, is estimated using Equation (20).

$$a^{\max}(t) = \frac{F_t(t) - R_t(t)}{m} \tag{16}$$

$$x_{\dot{u}} = \rho \cdot \nabla \cdot K_1 \tag{17}$$

$$K_1 = \frac{\alpha_0}{2 - \alpha_0} \tag{18}$$

$$\alpha_0 = \frac{2(1-e^2)}{e^3}\left[0.5 \ln\left(\frac{1+e}{1-e}\right) - e\right] \tag{19}$$

$$e = \sqrt{1 - \frac{\frac{3\nabla}{2\pi L/2}}{(L/2)^2}} \tag{20}$$

A simple linear ship-following model (as expressed in Equation (21)) is utilized to compute the safe inter-ship spacing, $s_n(t)$, under steady-state conditions. This spacing comprises the stopping distance, s_n^j (which is twice the ship length in this study). T_n represents the time required for the operator's reaction and the thrust deactivation process. T_n is estimated using Equation (22), where $L_c^{\max}$ is half the ship length and corresponds to the maximum signal travel distance, and u_s is the speed of sound, assumed to be 343 m/s. The reaction time, t_{pr}, varies with ship size and is typically set at 3.0 s for smaller vessels and 10.0 s for larger cargo ships.

$$s_n(t) = s_n^j + T_n u_n(t) \tag{21}$$

$$T_n = \frac{L_c^{max}}{u_s} + t_{pr} \tag{22}$$

$$\tilde{u}_n(t + \Delta t) = \min\left(\frac{s_n(t) - s_n^j}{T_n}, u_f\right) \tag{23}$$

Using Equation (21), the ship's following speed for the next time step, $\tilde{u}_n(t + \Delta t)$, is calculated as shown in Equation (23). The ship's speed is constrained by a maximum allowable speed, u_f, in the region. Additionally, the time-to-collision (TTC) is computed under the assumption of a constant current speed, as demonstrated in Equation (24).

$$TTC = \min\left(\frac{s_n(t) - s_n^j}{\max(u_n(t) - u_{n-1}(t), 0.0001)}, TTC_{\max}\right) \tag{24}$$

To predict the desired acceleration at a future time, two calculations are performed: one over the TTC interval (Equation (25)) and another over the T_n interval (Equation (27)). The maximum deceleration level, $d_{\max}$, due to resistance or reverse thrust, is estimated using Equation (26), incorporating a binary coefficient, β_0, which indicates the availability of reverse thrust.

$$a_{n,1-1}(t) = \max\left(\frac{\tilde{u}_n(t + \Delta t) - u_n(t)}{TTC}, -d_{max}\right) \tag{25}$$

$$d_{max} = \frac{R_t(t) + \beta_0 F_t(t)}{m} \tag{26}$$

$$a_{n,1-2}(t) = \min\left(\frac{\tilde{u}_n(t + \Delta t) - u_n(t)}{T_n}, a_n^{\max}(t)\right) \tag{27}$$

The ship acceleration is then determined as a weighted combination of these two values, with the binary term β_1 dictating whether the acceleration is negative or non-negative, as detailed in Equations (28) and (29). An alternate acceleration, based on the Lagrangian derivative of Equation (23), is calculated using Equation (30).

$$a_{n,1-3}(t) = (1 - \beta_1)a_{n,1-1}(t) + \beta_1 a_{n,1-2}(t) \tag{28}$$

$$\beta_1 = \frac{a_{n,1-1}(t) + |a_{n,1-1}(t)|}{2 \times \max(|a_{n,1-1}(t)|, 0.0001)} \tag{29}$$

We then compute the ship acceleration as a weighted combination of these two accelerations, where the term β_2 varies in the range [0,1]. The first acceleration term $(a_{(n,1-3)}(t))$ ensures that the ship spacing between it and the ship ahead complies with the range policy presented in Equation (23). The second acceleration term $(a_{(n,1-4)}(t))$ ensures that the ship adjusts its speed to the speed of the ship directly ahead of it. This is useful in case ships are following each other in a narrow canal similar to Suez canal, Egypt.

$$a_{n,1-4}(t) = \max\left(\min\left(\frac{u_{n-1}(t) - u_n(t)}{T_n}, a_n^{\max}(t)\right), -d_{max}\right) \tag{30}$$

The final acceleration $a_{n,1}(t)$ combines these components, balancing compliance with the range policy and adjustments to match the speed of the preceding ship. This method is

particularly relevant in constrained environments, such as the Suez Canal. Equation (31) expresses the weighted combination, with β_2 ranging between 0 and 1 to adjust the balance.

$$a_{n,1}(t) = \beta_2 a_{n,1-3}(t) + (1-\beta_2) a_{n,1-4}(t) \tag{31}$$

The longitudinal motion model extends the Fadhloun-Rakha car-following model [33,34] to incorporate ship dynamics. As shown in Equation (32), the model computes acceleration based on the relative velocities of the following and leading ships, ensuring smooth deceleration when approaching slower-moving vessels. The relevant parameters, including the deceleration level $d_{\max}$, are provided in Equation (33), with a binary variable γ handling speed conditions (Equation (34)).

$$a_n(t) = (1-\gamma) a_{(n,1)}(t) - \gamma a_{(n,2)}(t) \tag{32}$$

$$a_{n,2}(t) = \min\left(\frac{\left(u_n(t)^2 - u_{n-1}(t)^2\right)^2}{4\left(\max\left(s_n(t) - s_n^j - T_n u_n(t), 0.0001\right)\right)^2 d_{max}}, d_{max} \right) \tag{33}$$

$$\gamma = \frac{u_n(t) - u_{n-1}(t) + \sqrt{\left(u_n(t) - u_{n-1}(t)\right)^2}}{2 \times \max(|u_n(t) - u_{n-1}(t)|, 0.0001)} \tag{34}$$

When the spacing exceeds the threshold s_{lad}, defined in Equation (35), the ship is assumed to operate independently. The stopping distance x_{des} is determined through integration, considering resistance and reverse propulsion, as shown in Equation (36).

$$s_{lad} = s_{j_{n-1}} + x_{des} + s_n \tag{35}$$

$$x_{des} = \int_{v(t)}^{v(t)=0} (v(t) - d_{max} \cdot \Delta t) \cdot dt \tag{36}$$

Finally, smoothed acceleration $\widetilde{a}_n(t)$ is computed using an exponential smoother (Equation (37)), with the ship's speed updated iteratively via a first-order Euler approximation, as formulated in Equation (38). This comprehensive model ensures realistic simulation of ship-following behavior and operational dynamics.

$$\widetilde{a}_n(t) = \alpha \times a_n(t) + (1-\alpha) \times \widetilde{a}_n(t) \tag{37}$$

$$u_n(t + \Delta t) = \max\left(\min\left(u(t) + \widetilde{a}(t) \times \Delta t, u_f\right), 0\right) \tag{38}$$

4.3. Visibility Graph Modelling and Path Finding

This section is principally based on the work done by [36,37]. The purpose of this paper and the simulator is to study mainly long-voyage ships. For that, featuring the world map is essential to find the ships paths and mitigate obstacles. However, considering high/mid-resolution world maps with a large number of vertices slows down the simulator significantly. This slowness necessitates the use of the Quadtree in indexing the vertices by their location and hence makes it faster in searching and path-finding computations.

For simplicity, a world-Behrmann projected map is used. This simplification ensures faster calculations of distances between points. The map is further simplified into only points and lines instead of areas for faster indexing and shortest path planning. Considering the ship's depths, there may be areas with insufficient depths for the vessel. The simulator

allows for such adjustment as it transforms the shape points and lines to accommodate such consideration (Figure 2).

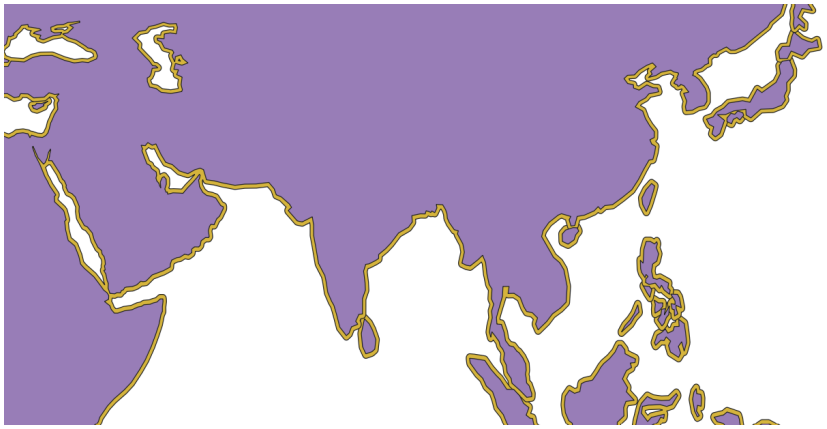

Figure 2. Transformation for depth considerations.

The main purpose of this module is to plan a path from the origin to the destination considering terrestrial formations as obstacles. The planning paths mostly contain the use of the visibility graph. This technique involves creating hypothetical links between the vertices/waypoints. Such linkages are, however, only possible in cases where the considered vertices are within mutual direct visual contact with each other and there are no obstacles in between. Hence, a constructed visibility graph—as this simplified visibility graph in Figure 3—should have about $\frac{n\times(n-1)}{2}$ links. After the visibility graph is constructed, a heuristic shortest path algorithm is applied for finding the best path. In this research, the heuristic function used is basically based on spatial distances as an example. However, the modification of the current heuristic consideration may be extended by including other factors, thereby increasing the adaptability of the algorithm in different navigational scenarios.

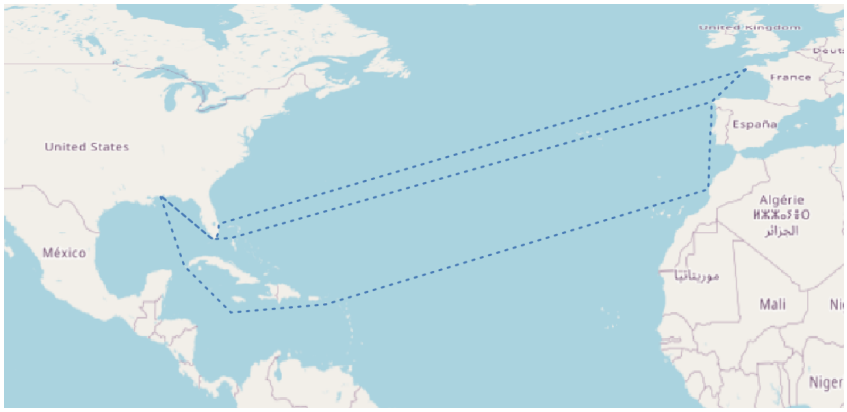

Figure 3. Simplified visibility graph between two points.

To further optimize the path planning processing efficiency, the QuadTree data structure is employed to index vertices/waypoints. The QuadTree excels in dividing a two-dimensional space, which enables quick querying and retrieval of points and faster checking of intersections. In this approach, each QuadTree node is recursively split into four quadrants as long as it contains more than one vertex. This approach reduces computational complexity in path planning by providing immediate access to specific vertices. As a result, the QuadTree speeds up the construction of visibility graphs and execution of shortest path algorithms.

5. Simulator Description

ShipNetSim is a simulation tool designed to model the movement of multiple ships within specified water boundaries. The simulator utilizes a longitudinal motion-based framework to simulate the propulsion and resistive forces acting on ships. It also incorporates ship-following models to determine ship behavior when they are in proximity to one another. The simulation operates on a time-driven algorithm, updating the movements of each vessel at every time step. Upon completion of the simulation, a summary file is generated that includes details such as the ships' travel time, distance traveled, energy consumption, fuel usage, and CO_2 emissions. Localization and trajectory computations are based on the ships' spatial coordinates, which gives potential for cyber-security studies as well. For additional details on simulating potential cyberattacks, see Section 5.

Moreover, the simulator is equipped to handle various fuel types. In this context, energy consumption primarily stems from the operational main engines of the ships. However, situations may arise where the engine's fuel source becomes depleted, rendering the engine inoperative. In such cases, the ship relies solely on resistive forces to decelerate until it comes to a complete stop.

Although the current study focuses exclusively on energy consumption from the main engine, the modular design of the simulator allows for extensions to account for energy consumption from auxiliary engines or generators.

The simulator structure (as illustrated in Figure 4) is divided into modules, each responsible for specific tasks. The network module defines the water boundaries, constructs the visibility graph, and manages pathfinding calculations. The ship dynamics module encapsulates ship characteristics, path trajectories, movement dynamics, and energy consumption. The central simulator module coordinates all calculations and manages the simulation of ship movements.

In the context of the visibility graph, the pathfinding module identifies paths as sequences of links and target points. Links are used to verify whether a ship can navigate a particular waterway based on its width, while points are treated as sequential waypoints. These links have conceptual widths constrained by the water body's boundaries. If a ship's width exceeds the width of a link, it is deemed unfit to pass through, simplifying conflict resolution and ship-following logic.

As shown in Figure 5, ShipNetSim initializes by specifying coordinates where ship speed must be zero, such as ports. If no specific stops are defined, a stop is automatically set at the route's endpoint. The primary condition driving the simulator is ensuring that all ships reach their designated destinations. The simulation concludes when all ships have arrived at their endpoints. A summary file is then generated, along with an optional trajectory file. If any ship has not yet reached its destination, the simulator identifies these ships and continues calculations specifically for them until all ships have completed their journeys.

At each time step (Figure 6), the simulator updates the current coordinates of each ship and gathers environmental data for that location. Using this information, it calculates the propulsion and resistance forces acting on the ship. The simulator also determines the maximum allowable speed for the region, if applicable, and calculates the distance to the next stop, reduced-speed zone, or nearby ship. This ensures that ships reduce speed appropriately to avoid collisions with other vessels or obstacles.

The collected data are passed to the ship dynamics module, which calculates the required acceleration or deceleration. The resultant speed is used to determine the incremental distance covered during the current time step. Energy consumption is then calculated based on the ship's characteristics. This process is repeated for all ships in the simulation.

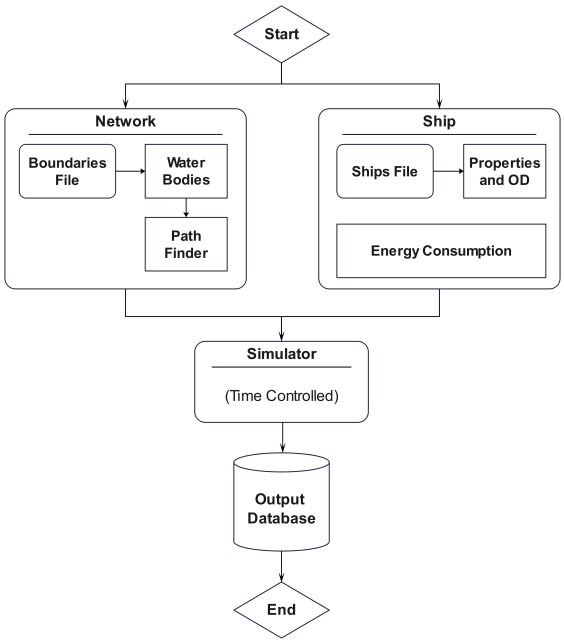

Figure 4. Simulator schema.

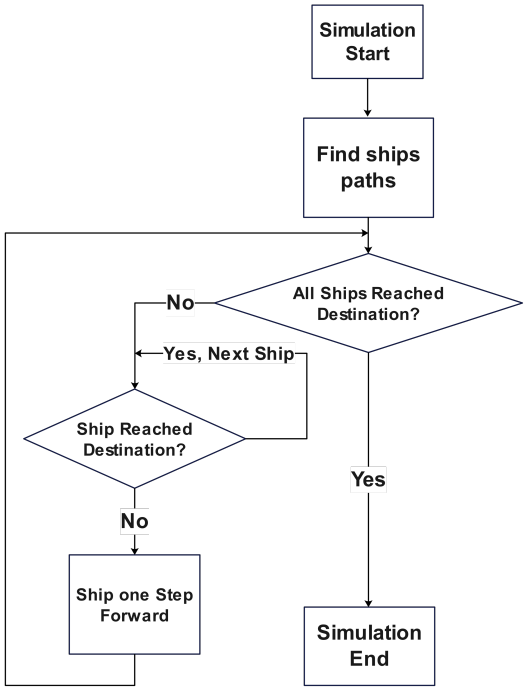

Figure 5. Simulator Flowchart.

Cybersecurity Simulation

As the maritime industry becomes more digitized and autonomous, the risk of cyber-attacks targeting critical ship systems, such as navigation, communication, and propulsion, is increasing. ShipNetSim is designed to model and simulate these cyber threats, especially the impacts of GPS spoofing, network attacks, and signal jamming. GPS spoofing can mislead the ship's navigation systems and its current GPS location, causing it to veer off course, which would result in inefficient routes, increased energy consumption, and higher fuel usage. ShipNetSim simulates such attacks by introducing randomized position offsets. Network-based attacks can disrupt communication between the ship and shore or between vessels. This can increase energy consumption as ships operate inefficiently due to delayed data or control commands or even increase the possibility of accidents. For autonomous

ships, the simulator can also model more complex cyberattacks, such as route manipulation, leading to dangerous or inefficient paths. ShipNetSim can simulate attacks that alter waypoints or introduce inefficiencies in pathfinding that would lead to less fuel efficiency and higher emissions. Additionally, it can model onboard system hacks that interfere with fuel control or throttle adjustments that lead to increased energy use or critical system failures. Beyond simulating attacks, ShipNetSim can be used to test mitigation strategies, such as encrypted communication or communication protocols and evaluate their effectiveness. Future developments could allow encryption of communication and integration of machine learning algorithms to predict potential cyberattacks. By incorporating these cybersecurity elements, ShipNetSim offers a comprehensive platform for understanding the impacts of cyber threats on ship operations, energy consumption, and emissions, while also providing insights into strategies to enhance the resilience of maritime systems.

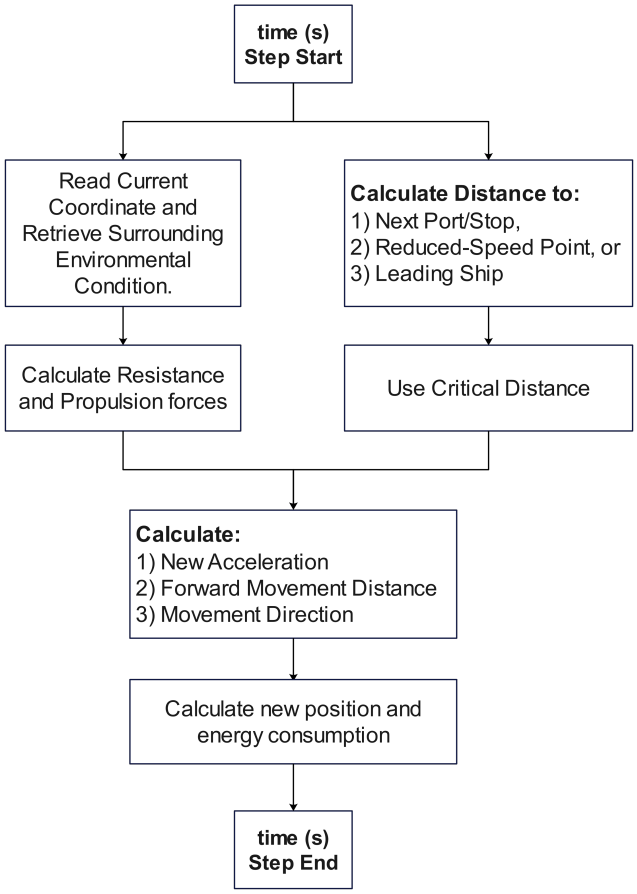

Figure 6. Time step simulation calculations.

6. Case Studies

This section presents a case study of modeling the S175 container ship (introduced in [38,39]) trajectory from Savannah, United States, to Algeciras, Spain. The simulator is capable of retrieving environmental characteristics per the vessel position needed for the resistance calculations. The environmental data are extracted from Geospatial tiff files provided by [40,41]. The vessel characteristics is provided in Table 1. The engine details and efficiency is retrieved from the engine manufacturer website [42]. This is the first attempt to validate the ShipNetSim's energy consumption capability. That is achieved by comparing the resultant energy consumption of the simulated ship against its reported average energy consumption. For this study, we used ShipNetSim version v0.0.1 and accessible from https://github.com/VTTI-CSM/shipNetSim/ (accessed on 13 May 2024).

Since the sources [40,41] provide neither the wave velocity nor wavelength, the wavelength is estimated using the below equation assuming water depth is always greater than $\lambda/2$ since in ocean environment:

$$\lambda = \frac{gT^2}{2\pi} \tag{39}$$

where λ is the wavelength in m, g is the gravitational acceleration in m/s^2, T is the wave period in s.

Table 1. Ship characteristics used in the case study.

Ship Characteristic	Value
Ship Name	S175
Route	Savannah, U.S. to Algeciras, Spain
Length between perpendiculars (m)	175
Beam (m)	25.4
Average Draft (m)	9.5
Design Speed (knot)	20
Displacement (m^3)	24,053
Block Coef	0.561
Prismatic coefficient	0.589
Position of LCG (m)	86.5
Fuel Type	HFO
Engine	6S60ME
Engine MCR @ L1 (kWh)	14,940
Engine RPM @ L1	105
Engine Eff at L1	0.5018
Propeller Diam (m)	5.0
Propeller Pitch (m)	4.75
Propeller Blade Count	5
Propeller Expanded Area Ratio	0.8
Weight (ton)	24,610.0

Figure 7 shows the ship speed-resistance profile of the ship. The travelled distance is shown on the x-axis, the speed in knots (represented by the solid line) on the left y-axis, and the total ship resistance in kN (represented by the dash line) on the right y-axis. Note that at high resistance values, the speed drops as the ship decelerates as a result of the significant increase in the resistance forces. For instance, at a distance of ∼700 nm, the speed drops from ∼20 kN to ∼18 kN due to a resistance of ∼300 kN.

Figure 8 provides visualization of the wave length (λ) and amplitude (ζ) fluctuations along the trajectory of the ship. These factors are significant in determining the resistance experienced by the vessel. This is because larger wave amplitudes increase the hydrodynamic pressure on the hull. In addition, the interaction of the ship with higher waves—particularly in head seas—leads to increased pitching. This disrupt the laminar flow around the hull and increases the drag and overall resistance significantly more than other resistance factors.

Wave length also has an influence on the ship resistance through its effect on the ship motion (pitching and heaving). When the the wave length resonate with the ship length ($l_{pp}/\lambda \approx 1.0$), it can exaggerate these motions and hence increase resistance similar to what happened at 1300 nm.

The simulation results show that the ship reached its destination in 7 days and 15 h with a total energy consumption of 478 tons of heavy fuel oil and ∼1495 tons of carbon dioxide emissions with a fuel density of 1010 kg/m^3 and calorific value of 40.9 MJ/kg. The total energy consumption of the same ship is reported in [43] as a rough estimate to be ∼550 tons for an approximate-equivalent voyage. This is equivalent to a difference of 13.09% demonstrating that the model produces reasonable fuel consumption estimates.

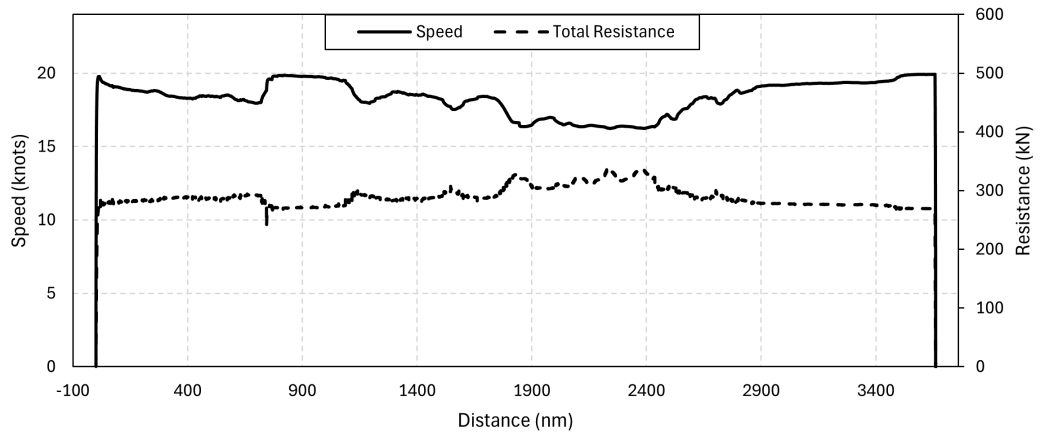

Figure 7. Speed vs. resistance profile of the ship.

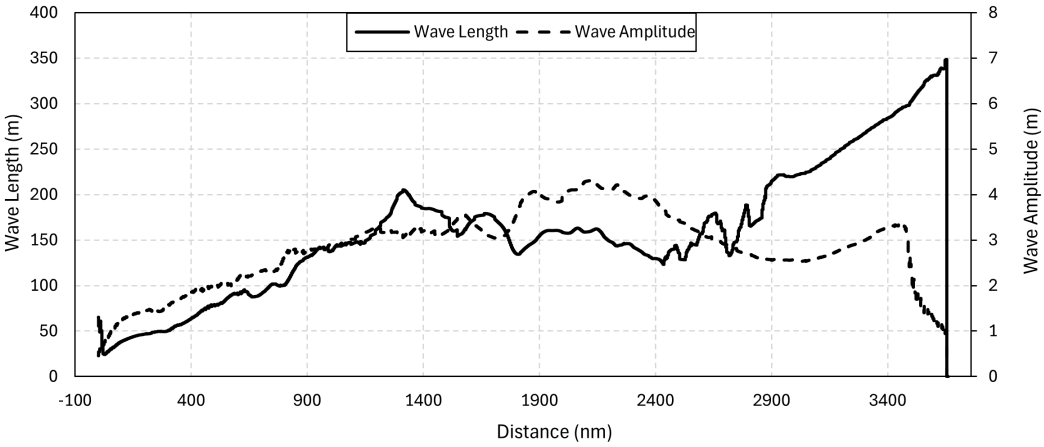

Figure 8. Wave characteristics along ship trajectory.

6.1. Environment Sensitivity Analysis

In this section, we examine the sensitivity of the model to the environmental variations by simulating the ship's voyage across different monthly conditions from November 2023 to October 2024. The analysis was conducted to observe how these conditions affect the vessel's fuel consumption.

This entailed running the simulation with the environmental conditions captured at the beginning of every month. Results have shown that resistance forces affecting the fuel consumption which the ship encountered varied between 463.68 to 483.70 tons. Table 2 summarizes the outcomes of each simulated month and points out the corresponding heavy fuel oil (HFO) consumption for each voyage. The average fuel consumption across these months was about 473.24 tons, with a standard deviation of 7.13 tons (1.5% of the mean), reflecting minor variability due to monthly environmental changes.

The ship's experienced resistance forces required slight increases in fuel consumption during higher resistance months, which affected operational efficiency. This variability in fuel consumption across the months illustrates the correlation between environmental resistance and fuel usage, with slightly more fuel required during periods with less favorable conditions. During months with comparatively lower resistance, the engine maintained its power output with minimal external forces, resulting in optimized fuel usage and efficiency.

For comparative purposes, an additional simulation was conducted under idealized environmental conditions (no open-sea environmental considerations), producing an HFO consumption of 456.42 tons—a difference of 3.55% compared to the monthly mean value. This serves as a benchmark to pinpoint the fuel savings under optimal conditions with

minimal resistance. The idealized scenario provides a reference for the lowest possible fuel consumption achievable by this ship in the absence of external environmental resistive forces.

Table 2. Environment sensitivity analysis results for S175 container ship (November 2023–October 2024).

Date	HFO Consumption (tons)
Nov. 2023	478.22
Dec. 2023	471.06
Jan. 2024	482.85
Feb. 2024	463.68
Mar. 2024	480.17
Apr. 2024	483.70
May 2024	478.07
Jun. 2024	468.89
Jul. 2024	466.27
Aug. 2024	468.15
Sep. 2024	464.79
Oct. 2024	473.03
Ideal Conditions	456.42

6.2. Discussion and Comparison

The findings of the simulation of the S175 container vessel show that ShipNetSim correctly forecasts main operational parameters, with a calculated consumption of 478 tons of heavy fuel oil and nearly 1495 tons of CO_2 emissions during a 7-day, 15 h voyage within a 13.1% margin of error compared to the reported theoretically calculated operational statistics [43]. The degree of accuracy apparent in these observations suggests that the integrative methodology—of sophisticated hydrodynamic modeling, dynamic ship-following routines, and real-time weather data—provides a sound foundation for maritime energy consumption and emissions computation using simulation.

One of the key strengths of ShipNetSim is its comprehensive multi-domain scope. Unlike conventional simulators that tend to separate elements of vessel motion or energy calculation, our system integrates these variables with the addition of a cybersecurity module that has been developed specifically to model digital disruptions. The integrated approach enables a broad evaluation of operational effectiveness while new maritime cyber resilience problems are being dealt with simultaneously, effectively broadening the application of the simulator to ongoing decarbonization initiatives and regulatory compliance programs.

In spite of these strengths, several limitations are worthy of mention. First, ShipNetSim is specialized to longitudinal dynamics only at present, simplifying the computational model; however, this specialization may fail to properly represent lateral interactions or three-dimensional maneuvering behavior in confined spaces. Second, the intricacy involved in the full equations—although valuable for reproducibility—may reduce the simulator's usability for researchers who prefer an easier-to-use tool. These aspects point to possible directions for future development, like the addition of lateral motion features and the improvement of the user interface.

6.3. Analysis of Model Uncertainties

Although no formal uncertainty quantification analysis was conducted in this study, some probable sources of uncertainty intrinsic to ShipNetSim have been recognized. They are:

- Variability of Environmental Data: The simulation relies on environmental data (e.g., geospatial tiff files for wind and wave parameters) that inherently contain measurement errors and temporal/spatial variability.
- Model Parameter Calibration: Key parameters like the calibration coefficients (t_1, t_2, t_3) and the form factor (k_1) are derived from empirical data and literature values, which can be different in operating conditions.
- Numerical Approximations: The use of discrete time steps (Δt) and numerical integration techniques can lead to approximation errors.

In spite of such possible uncertainties, the simulation results bear a significant resemblance to the operational figures that have been recorded. For instance, the estimated fuel consumption of the S175 container ship was within 13.1% of the figure that was actually recorded, and the sensitivity analysis conducted on twelve monthly scenarios revealed merely a 1.5% deviation in fuel consumption. Such findings indicate that, for the present configuration, the overall impact of uncertainties is minimal. Future work will try to include formal approaches to uncertainty quantification, i.e., Monte Carlo simulations, in order to give a more complete statistical characterization of the model uncertainties.

7. Conclusions

This paper introduces ShipNetSim. The open-source simulator is designed for analyzing marine fuel consumption, energy use, and greenhouse gas emissions in multi-vessel scenarios. ShipNetSim employs motion-based modeling, integrating vessel coexistence strategies derived from traffic flow theory with vessel motion dynamics to simulate longitudinal behavior. The simulator generates various metrics, including instantaneous acceleration, velocity, position, energy and fuel consumption, and CO_2 emissions for all vessels within the simulated network. Currently, the simulator focuses exclusively on longitudinal motion; however, future enhancements will aim to incorporate lateral movement.

In this paper, we present ShipNetSim, a unique open-source multi-vessel simulator for the quantification of marine fuel, energy, and greenhouse gas emissions. ShipNetSim is a motion-based simulator that uses vessels coexistence strategies adapted from traffic flow theory in combination with vessel motion modelling to model the longitudinal motion behavior of vessels. The simulator outputs consist of different metrics such as the instantaneous acceleration levels, speeds, position, fuel/energy consumption, CO_2 emissions of all vessels in the simulated network. As of now, the simulator only considers the longitudinal motion of the vessel; nonetheless, future work entails incorporating side movement as well.

In addition, ShipNetSim has a significant potential to inform environmental policy and regulatory compliance. The simulator provides a basis for assessing various operating tactics with regard to how effective they are in relation to international maritime policies—for instance, carbon-reduction goals of the International Maritime Organization, which are driving towards efficiency and emission reduction. The above quantification of emissions by the simulator and energy consumption enables shipping companies and policy-makers to weigh vessel operations' environmental impact and decide on the best way to implement green shipping practices. By simulating scenarios such as speed adjustments, optimized routing, or the use of alternative fuels, ShipNetSim can play a major role in helping stakeholders achieve compliance with evolving global sustainability targets. The flexibility of the simulator ensures that it can be adapted to future policy changes, making it a go-to tool for both the maritime industry and regulatory bodies looking to mitigate the environmental footprint of shipping operations.

In spite of these promising findings, there are a number of research gaps that need to be filled through further research. Specifically, the existing version of ShipNetSim is limited to studying longitudinal dynamics alone. Future research efforts should extend

the model to lateral motion and comprehensive three-dimensional maneuvering to reach a more comprehensive understanding of ship dynamics. Additionally, while our simulation findings are in very good alignment with operational data, the inclusion of formal uncertainty quantification techniques can potentially enhance the credibility of our projections even more. Finally, there is tremendous opportunity to explore more sophisticated cyber threat modeling (e.g., real-time vessel-to-vessel and vessel-to-shore communications) and the adoption of hybrid propulsion systems and alternative fueling strategies in support of enabling decarbonization in maritime transportation. The closure of these loopholes will continue to enhance ShipNetSim as an essential tool for green shipping operations and policy development.

Future research will expand ShipNetSim's capabilities to include additional ship motion dynamics and more detailed cyber threat modeling. This will further increase its value for optimizing ship performance and ensure secure and efficient maritime operations.

Author Contributions: Study conception and design, analysis and interpretation of results, software development, and writing: A.A.; study conception, funding, advising, interpretation of results, editing the final draft: H.A.R. All authors reviewed the results and approved the final version of the manuscript.

Funding: This research was supported by the Sustainable Mobility and Accessibility Regional Transportation Equity Research Center at Morgan State University and the University Transportation Center(s) Program of the U.S. Department of Transportation under fund number 69A3552348303. The views and opinions of authors expressed herein do not necessarily state or reflect those of the United States Government or any agency thereof.

Data Availability Statement: ShipNetSim is an open-source simulation software accessible from https://github.com/VTTI-CSM/shipNetSim/. Further inquiries can be directed to the corresponding author.

Conflicts of Interest: The authors declare no conflict of interest.

Abbreviations

Variable	Definition
$\tilde{a}_n(t)$	Smoothed acceleration of ship n at instant t (m/s^2)
$a_n(t)$	Acceleration of ship n at instant t (m/s^2)
B	Ship Beam (m)
$F_{t\|n}(t)$	Propulsion force of ship n at instant t (N)
$Fr(t)$	The Froude number at instant t
P_l^{max}	Maximum engine power of the main engine (kW)
T_n	The time it takes to deactivate the propulsion thrust or revert the propeller rotating direction plus the operator perception reaction time (s)
L_{PP}	The ship length between perpendiculars (m)
m	Total mass of the vessel (kg)
$R_{t\ midn}(t)$	Total Resistive forces at instant t (N)
$R_{CALM}(t)$	The calm water resistance component at instant t (N)
$R_{AW}(t)(\omega(t)\|u(t),\beta(t))$	The added resistance component due to waves of frequency ω and wave heading angle β at instant t (N)
$R_{awr}(t)(\omega(t)\|u(t),\beta(t))$	The added resistance component due to wave reflection with wave frequency ω and wave heading angle β at instant t (N)

$R_{awm}(\omega(t)\|u(t),\beta(t))$	The added resistance component due to the ship motion with wave frequency ω and wave heading angle β at instant t (N)
$R_{awr}(t)(\omega(t)\|u(t),0)$	The added resistance component due to wave reflection with wave frequency ω and wave heading angle β in the longitudinal heading direction at instant t (N)
$R_{awm}(\omega(t)\|u(t),0)$	The added resistance component due to the ship motion with wave frequency ω and wave heading angle β in the longitudinal heading direction at instant t (N)
$R_{AA}(t)$	The added resistance component due to wind at instant t (N)
$R_F(t)$	The calm-water frictional resistance component at instant t (N)
$R_W(t)$	The calm-water wave-making resistance component at instant t (N)
$R_W(t)$	The calm-water bulbus bow resistance component at instant t (N)
$R_{TR}(t)$	The calm-water transom resistance component at instant t (N)
$R_A(t)$	The calm-water model correction resistance component at instant t (N)
k_1	The form factor of the ship
ρ_A	The air density (kg/m^3)
C_{AA}	The wind resultant resistance coefficients (of $C_{AA\|x}$ and $C_{AA\|y}$) for various wind heading angle ψ
$C_{AA\|x}$	The wind resistance coefficients in the longitudinal direction for various wind heading angle ψ
$C_{AA\|y}$	The wind resistance coefficients in the lateral direction for various wind heading angle ψ
$\psi(t)$	The heading angle of the wind at instant t
A_{XV}	The transverse projected area above waterline including superstructures (m^2)
$V^2_{WR}(t)$	The relative wind speed at instant t
X_i&$Y_i, i \in [0,...,5]$	The coefficients for estimating C_{AA}.
$s_n(t)$	Distance between the stern of ship n and the stern of ship $n-1$, calculated as $x_{n-1}(t) - x_n(t)$ (m)
s^j_n	Minimum allowable spacing (m), equal to the length of ship n plus a buffer (assumed to be equal to the ship's length)
t_1, t_2, t_3	Throttle input coefficients
$u_d(t)$	Target speed or the maximum allowable speed for a ship at time t (m/s)
u_f	Maximum permissible speed in the given environment (km/h)
$u_m(t)$	Speed achieved by the ship at full throttle at time t (m/s)
$u_n(t)$	Speed of ship n at instant t (m/s)
λ^*	Throttle setting that balances resistance forces at instance t, constrained within $(0 \leq \lambda \leq 1)$
$\lambda(t)$	Throttle level at time t, constrained within $(0 \leq \lambda \leq 1)$
Δt	Time step for numerical solutions (s)
g	Gravitational acceleration (9.8066 m/s^2)
η_n	Mechanical efficiency of the main engine of ship n
$z(t)$	depth from sea level at instant t (m)
$\zeta_a(t)$	the wave amplitude at instant t (m)

References

1. Sato, Y.K.; Miyata, H.; Sato, T. CFD simulation of 3-dimensional motion of a ship in waves: Application to an advancing ship in regular heading waves. *J. Mar. Sci. Technol.* **2000**, *4*, 108–116. [CrossRef]
2. Ueng, S.; Lin, D.; Liu, C.H. A ship motion simulation system. *Virtual Real.* **2008**, *12*, 65–76. [CrossRef]
3. Zhang, W.; Zou, Z.; Deng, D.h. A study on prediction of ship maneuvering in regular waves. *Ocean. Eng.* **2017**, *137*, 367–381. [CrossRef]
4. Yum, K.K.; Tavakoli, S.; Bø, T.A.; Nielsen, J.B.; Stenersen, D. Design Lab: A simulation-based approach for the design of sustainable maritime energy systems. In Proceedings of the International Marine Design Conference, Delft, The Netherlands, 2–6 June 2024. [CrossRef]
5. Visky, G.; Lavrenovs, A.; Orye, E.; Heering, D.; Tam, K. Multi-Purpose Cyber Environment for Maritime Sector. In Proceedings of the International Conference on Cyber Warfare and Security, New York, NY, USA, 17–18 March 2022. [CrossRef]
6. Tam, K.; Forshaw, K.; Jones, K. Cyber-SHIP: Developing Next Generation Maritime Cyber Research Capabilities. In Proceedings of the Conference Proceedings of ICMET Oman, Muscat, Oma, 5–7 November 2019. [CrossRef]
7. Antonopoulos, M.; Drainakis, G.; Ouzounoglou, E.; Papavassiliou, G.; Amditis, A. Design and proof of concept of a prediction engine for decision support during cyber range attack simulations in the maritime domain. In Proceedings of the 2022 IEEE International Conference on Cyber Security and Resilience (CSR), Rhodes, Greece, 27–29 July 2022; pp. 305–310. [CrossRef]
8. Mrakovic, I.; Vojinović, R. Maritime Cyber Security Analysis—How to Reduce Threats? *Trans. Marit. Sci.* **2019**, *8*, 132–139. [CrossRef]
9. Sasa, K.; Chen, C.; Fujimatsu, T.; Shoji, R.; Maki, A. Speed loss analysis and rough wave avoidance algorithms for optimal ship routing simulation of 28,000-DWT bulk carrier. *Ocean. Eng.* **2021**, *228*, 108800. [CrossRef]
10. Chen, C.; Chen, X.Q.; Ma, F.; Zeng, X.J.; Wang, J. A knowledge-free path planning approach for smart ships based on reinforcement learning. *Ocean. Eng.* **2019**, *189*, 106299. [CrossRef]
11. Xue, Y.; Clelland, D.; Lee, B.S.; Han, D. Automatic simulation of ship navigation. *Ocean. Eng.* **2011**, *38*, 2290–2305. [CrossRef]
12. Calleya, J.; Pawling, R.; Greig, A. Ship impact model for technical assessment and selection of Carbon dioxide Reducing Technologies (CRTs). *Ocean. Eng.* **2015**, *97*, 82–89. [CrossRef]
13. Işıklı, E.; Aydın, N.; Bilgili, L.; Toprak, A. Estimating fuel consumption in maritime transport. *J. Clean. Prod.* **2020**, *275*, 124142. [CrossRef]
14. Jensen, S.; Lützen, M.; Mikkelsen, L.L.; Rasmussen, H.B.; Pedersen, P.V.; Schamby, P. Energy-efficient operational training in a ship bridge simulator. *J. Clean. Prod.* **2018**, *171*, 175–183. [CrossRef]
15. Luo, X.; Wang, M. Study of solvent-based carbon capture for cargo ships through process modelling and simulation. *Appl. Energy* **2017**, *195*, 402–413. [CrossRef]
16. Yun, P.E.; Xiangda, L.I.; Wenyuan, W.A.; Ke, L.I.; Chuan, L.I. A simulation-based research on carbon emission mitigation strategies for green container terminals. *Ocean. Eng.* **2018**, *163*, 288–298. [CrossRef]
17. Mocerino, L.; Soares, C.G.; Rizzuto, E.; Balsamo, F.; Quaranta, F. Validation of an Emission Model for a Marine Diesel Engine with Data from Sea Operations. *J. Mar. Sci. Appl.* **2021**, *20*, 534–545. [CrossRef]
18. Lebedevas, S.; Čepaitis, T. Complex Use of the Main Marine Diesel Engine High- and Low-Temperature Waste Heat in the Organic Rankine Cycle. *J. Mar. Sci. Eng.* **2024**, *12*, 521. [CrossRef]
19. Liu, J.; Duru, O. Bayesian probabilistic forecasting for ship emissions. *Atmos. Environ.* **2020**, *231*, 117540. [CrossRef]
20. Thiaucourt, J.; Horel, B.; Tauzia, X.; Ncobo, C. Numerical investigation to increase ship efficiency in regular head waves using an alternative engine control strategy. *Proc. Inst. Mech. Eng. Part M* **2023**, *237*, 436–454. [CrossRef]
21. Hai, T.; Basem, A.; Shami, H.O.; Sabri, L.S.; Rajab, H.; Farqad, R.O.; Hussein, A.H.A.; Alhaidry, W.A.A.L.H.; Idan, A.H.; Singh, N.S.S. Utilizing the thermal energy from natural gas engines and the cold energy of liquid natural gas to satisfy the heat, power, and cooling demands of carbon capture and storage in maritime decarbonization: Engineering, enhancement, and 4E analysis. *Int. J. Low Carbon Technol.* **2024**, *19*, 2093–2107. [CrossRef]
22. Ammar, N.R.; Seddiek, I.S. Enhancing sustainability in LNG carriers through integrated alternative propulsion systems with Flettner rotor assistance. *Brodogradnja* **2025**, *76*, 76102. [CrossRef]
23. Aredah, A.; Rakha, H.A. ShipNetSim: A Multi-Ship Simulator for Evaluating Longitudinal Motion, Energy Consumption, and Carbon Footprint of Ships. In Proceedings of the 2024 IEEE International Conference on Smart Mobility (SM), Niagara Falls, ON, Canada, 16–18 September 2024; pp. 116–121. [CrossRef]
24. Aredah, A.; Rakha, H. *Energy Consumption Modeling of Ships: Towards a Door-to-Door (D2D) Freight Optimization*; Technical Report for Sustainable Mobility and Accessibility Regional; Morgan State University: Baltimore, MD, USA, 2024.
25. Aredah, A.; Du, J.; Hegazi, M.; List, G.; Rakha, H.A. Comparative analysis of alternative powertrain technologies in freight trains: A numerical examination towards sustainable rail transport. *Appl. Energy* **2024**, *356*, 122411. [CrossRef]
26. Tavakoli, S.; Najafi, S.; Amini, E.; Dashtimansh, A. Ship acceleration motion under the action of a propulsion system: A combined empirical method for simulation and optimisation. *J. Mar. Eng. Technol.* **2021**, *20*, 200–215. [CrossRef]

27. Lang, X.; Mao, W. A semi-empirical model for ship speed loss prediction at head sea and its validation by full-scale measurements. *Ocean. Eng.* **2020**, *209*, 107494. [CrossRef]
28. Fujiwara, T.; Ueno, M.; Nimura, T. Estimation of Wind Forces and Moments acting on Ships. *J. Soc. Nav. Archit. Jpn.* **1998**, *1998*, 77–90. [CrossRef]
29. Lewis, E.V. *Principles of Naval Architecture: Volume II—Resistance, Propulsion and Vibration*, 2nd ed.; The Society of Naval Architects and Marine Engineers: Jersey City, NJ, USA, 1988.
30. *ISO 15016:2025*; Marine Technology—Guidelines for the Assessment of Speed and Power Performance by Analysis of Speed Trial Data. ISO: Geneva, Switzerland, 2025.
31. Strom-Tejsen, J. Added resistance in waves. *Soc. Nav. Archit. Mar. Eng.* **1973**, *8*, 109–143.
32. Yehia, W.; Moustafa, M.M. Practical considerations for marine propeller sizing. In Proceedings of the International Marine and Offshore Engineering Conference, Lisbon, Portugal, 15–17 October 2014.
33. Fadhloun, K.; Rakha, H. A novel vehicle dynamics and human behavior car-following model: Model development and preliminary testing. *Int. J. Transp. Sci. Technol.* **2020**, *9*, 14–28. [CrossRef]
34. Aredah, A.S.; Fadhloun, K.; Rakha, H.A. NeTrainSim: A network-level simulator for modeling freight train longitudinal motion and energy consumption. *Railw. Eng. Sci.* **2024**, *32*, 480–498. [CrossRef]
35. Zeraatgar, H.; Moghaddas, A.; Sadati, K. Analysis of surge added mass of planing hulls by model experiment. *Ships Offshore Struct.* **2020**, *15*, 310–317. [CrossRef]
36. Lee, W.; Choi, G.H.; Kim, T.w. Visibility graph-based path-planning algorithm with quadtree representation. *Appl. Ocean. Res.* **2021**, *117*, 102887. [CrossRef]
37. Wu, G.; Atilla, I.; Tahsin, T.; Terziev, M.; Wang, L. Long-voyage route planning method based on multi-scale visibility graph for autonomous ships. *Ocean. Eng.* **2021**, *219*, 108242. [CrossRef]
38. Lang, X.; Mao, W. A Practical Speed Loss Prediction Model at Arbitrary Wave Heading for Ship Voyage Optimization. *J. Mar. Sci. Appl.* **2021**, *20*, 410–425. [CrossRef]
39. Zhao, F.; Yang, W.; Tan, W.W.; Chou, S.K.; Yu, W. An overall ship propulsion model for fuel efficiency study. *Energy Procedia* **2015**, *75*, 813–818. [CrossRef]
40. E.U. Copernicus Marine Service Information (CMEMS). Global Ocean Hourly Sea Surface Wind and Stress from Scatterometer and Model. Available online: https://data.marine.copernicus.eu/product/WIND_GLO_PHY_L4_NRT_012_004/description (accessed on 13 May 2024).
41. E.U. Copernicus Marine Service Information (CMEMS). Global Ocean Physics Analysis and Forecast. Available online: https://data.marine.copernicus.eu/product/GLOBAL_ANALYSISFORECAST_PHY_001_024/description (accessed on 13 May 2024).
42. MAN. CEAS Engine Calculations. Available online: https://www.man-es.com/marine/products/planning-tools-and-downloads/ceas-engine-calculations (accessed on 25 May 2024).
43. Huotari, J.; Manderbacka, T.; Ritari, A.; Tammi, K. Convex optimisation model for ship speed profile: Optimisation under fixed schedule. *J. Mar. Sci. Eng.* **2021**, *9*, 730. [CrossRef]